

# Simulations of polarization from accretion disks

**J. Schultz**

000014 University of Helsinki, Observatory, P.O. Box 14, Finland (juho.schultz@astro.helsinki.fi)

Received 17 January 2000 / Accepted 19 October 2000

**Abstract.** The Monte Carlo Method was used to estimate the level of polarization from axisymmetric accretion disks similar to those in low-mass X-ray binaries and some classes of cataclysmic variables. In low-mass X-ray binaries electron scattering is supposed to be the dominant opacity source in the inner disk, and most of the optical light is produced in the disk. Thompson scattering occurring in the disk corona produces linear polarization. Detailed theoretical models of accretion disks are numerous, but simple mathematical disk models were used, as the accuracy of polarization measurements does not allow distinction of the fine details of disk models. Stokes parameters were used for the radiative transfer. The simulations indicate that the vertical distribution of emissivity has the greatest effect on polarization, and variations of radial emissivity distribution have no detectable effect on polarization. Irregularities in the disk may reduce the degree of polarization. The polarization levels produced by simulations are detectable with modern instruments. Polarization measurements could be used to get rough constraints on the vertical emissivity distribution of an accretion disk, provided that a reasonably accurate disk model can be constructed from photometric or spectroscopic observations in optical and/or X-ray wavelengths.

**Key words:** accretion, accretion disks – polarization – methods: numerical

## 1. Introduction

Solving the radiative transfer equation for each of the four Stokes parameters is not straightforward, and complicated geometries often lead to extremely complicated equations. Therefore numerical methods, such as the Monte Carlo method (see e.g. Cashwell & Everett 1959), are often used to approximate the solution. Monte Carlo simulations have been used to estimate the polarization levels of axisymmetric systems, such as galaxies (Bianchi et al. 1996) and disks around Be stars (Wood et al. 1996). I have used the Monte Carlo method to simulate the polarization of axisymmetric pure electron scattering accretion disks. These disks are similar to those observed in two types of low-mass X-ray binaries (LMXB:s): Z sources and soft X-ray transients (SXT:s) in outburst. These systems have high mass

accretion rates and X-ray luminosities. In LMXB:s the outer accretion disk is heated by the X-rays from the compact star and the inner accretion disk. X-rays heat the disk often to temperatures above the hydrogen ionization temperature (King et al. 1997). Therefore in systems with high accretion rates the disk is completely ionized.

Only very few observations of linear polarization from LMXB:s have been published. (Dolan & Tapia 1989) have observed the transient source A0620-00, and (Egonsson & Hakala 1991) have observed the eclipsing system Her X-1. In both systems the polarization was variable with amplitudes  $\sim 1.5\%$  for A0620-00 and  $\sim 0.3\%$  for Her X-1. Older observations (Shakhovskoi & Efimov 1975 and references therein) have lower signal to noise ratios. However, Shakhovskoi & Efimov report variable linear polarization from Sco X-1 with an amplitude of  $\sim 1\%$ .

The simulations produced polarization levels of the order 1% in white light. The geometry of the radiating area was the most important factor affecting the polarization. My results indicate that if a disk model can be constructed on the basis of other observations, some on constraints vertical emissivity structure can be derived from polarization measurements.

## 2. The Monte Carlo code

My code follows closely the procedure described in Bianchi et al. (1996). The simulation is made in the following way:

1. Emission: Random place and direction of an unpolarized (pseudo)photon is calculated from the brightness distribution of the disk.
2. A random optical depth is selected, and the photon path in the disk is integrated until this optical depth is reached.
3. Scatter the photon and return to step 2, until the photon exits the disk.
4. The photon Stokes parameters are added to those of the corresponding inclination bin.
5. Return to step 1, until enough photons have been calculated.

The coordinates of the photon emission place in cylindrical coordinates, with  $z = 0$  in the disk plane, are calculated from three random numbers  $R_i$ :

$$R_1 = F(r) = \frac{\int_{r_{\min}}^r \epsilon(r') r' dr'}{\int_{r_{\min}}^{r_{\max}} \epsilon(r') r' dr'} \quad (1)$$

$$R_2 = G(z, r) = \frac{\int_{z(r)_{\min}}^z \epsilon(z') dz'}{\int_{z(r)_{\min}}^{z(r)_{\max}} \epsilon(z') dz'} \quad (2)$$

$$\phi = 2\pi R_3 \quad (3)$$

where  $\epsilon$  and  $\varepsilon$  are the functions describing the emissivity distribution. From the form of Eq. (1) and Eq. (2), it is clear that  $\epsilon$  and  $\varepsilon$  should be simple enough to allow direct calculation of  $F(r)$  and  $G(z, r)$ , or  $F(r)$  and  $G(z, r)$  should be tabulated. The limits of the integral in Eq. (2) are dependent on radius. To solve this problem efficiently, the limits are set by selected values of vertical optical depth, defined by

$$\tau(z) = \int_z^\infty \kappa_r \rho(r, z') dz' \quad (4)$$

Now two values of vertical optical depth,  $\tau_{1,2}$ , are selected. All photons are emitted between these. This parametrization is made to help distinguishing between different energy sources. It is important to restrict the emission to layers near the disk surface, as the optical depth from the disk plane is very large, of the order 10000, in the inner disk. Otherwise most of the computing effort would go to modelling the radiative transfer in the disk plane, which is irrelevant for the polarization of observed radiation. Also, the polarization of radiation from  $\tau(z) > 10$  is saturated, i.e. it is consistent with the Chandrasekhar solution of semi-infinite slab (Wood et al. 1996).

Some of the scattered photons travel to the disk plane, reaching very large optical depth values. They scatter around in the deeper layers and most of them will never exit the disk. If these photons are not eliminated from the simulation, most of the time is spent for their radiative transfer, which is also irrelevant for observed polarization. Therefore all photons crossing the bottom of the radiating layer are discarded.

$$\tau_1 = \int_{z(r)_{\max}}^\infty \kappa_r \rho(r, z') dz' \quad (5)$$

$$\tau_2 = \int_{z(r)_{\min}}^\infty \kappa_r \rho(r, z') dz' \quad (6)$$

From these the vertical optical depth corresponding to random place between  $\tau_1$  and  $\tau_2$  can be calculated.

$$R_2 = \frac{\tau_z - \tau_1}{\tau_2 - \tau_1} \quad (7)$$

Substituting  $\tau_z$  to Eq. (4),  $z$  can be solved. To simplify the calculations, I adopt exponential vertical structure,  $\rho(r, z) = \rho_{\text{plane}}(r) \exp(-z/H)$ , so that Eq. (4) can be inverted analytically.

From the above equations, the three coordinates of a random emission place corresponding to some emissivity and density distribution can be solved.  $\epsilon = CR^\gamma$  and  $\varepsilon = \text{constant}$  were used. The inner disk radius,  $R_{\min}$ , was set to one, and the maximum radius,  $R_{\max}$ , was set to a value corresponding to the outer

edge of the simulated disk model, and  $\tau_{1,2}$  were set to constant values.

The direction angles of the emitted photon are calculated from  $\varphi = 2\pi R_4$  and  $\cos \theta = 2R_5 - 1$  where  $R_{4,5}$  are random numbers. After emission, the photon travels to a random optical depth  $\tau$ , which is calculated from

$$\tau = -\ln(1 - R_6) \quad (8)$$

When the optical depth  $\tau$  and direction  $S(\theta, \varphi)$  to which the photon travels, are known, the density distribution can be integrated until either  $\tau$  is reached or the photon exits the disk. Formally this can be expressed as

$$\tau = \int \kappa_r \rho(r, z) dS \quad (9)$$

If the photon is still in the disk, three more random numbers are required, two to obtain the scattering direction  $(\theta_s, \varphi_s)$ .

$$S_1 = \frac{1}{2} - \frac{3 \cos \theta_s}{8} - \frac{\cos^3 \theta_s}{8} \quad (10)$$

$$S_2 = \frac{\varphi_s}{2\pi} + \frac{P}{8\pi} \sin^2 \theta \sin 2\varphi_s \quad (11)$$

where  $P = \sqrt{Q^2 + U^2}/I$  is the degree of polarization before scattering, and  $\varphi_s$  is measured from the direction of incident ray polarization. The third random number is needed for calculating the new optical depth from Eq. (8). A total of  $6 + 3N$  random numbers are required for a photon scattering  $N$  times.

The Stokes parameters of each photon exiting to a specific inclination interval are summed to get the approximate solution for the radiative transfer. The mean error of the mean of the Stokes Q and U parameters can be calculated for each inclination bin from:

$$\sigma_Q = \sqrt{\frac{\sum_{i=1}^N (Q_i - (1/N)(\sum_{j=1}^N Q_j))^2}{N(N-1)}} \quad (12)$$

Where the summations with indices  $i$  and  $j$  include all photons in the bin, and  $N$  is the number of photons in the bin. Eq. (12) has one significant drawback: The double sum can not be computed, unless all the Stokes parameters of each photon are known. This reduces the efficiency of simulations severely. If  $N$  is large, the error can be approximated by expanding the square in Eq. (12), and setting the term with highest power of  $1/N$  to zero. The small negative term left inside the square root is divided by two to prevent any artificial decrease of the error estimate. The new error estimate is:

$$\sigma_Q = \sqrt{\frac{\sum_{i=1}^N Q_i^2 - (1/N)(\sum_{i=1}^N Q_i)^2}{N(N-1)}} \quad (13)$$

This has also been used in (Wood et al. 1996) to estimate the errors of the simulation. The sums in Eq. (13) can be calculated during the simulation, as the double summation vanishes. The error of Stokes I is insignificant when compared to the errors of Q and U.

I tested the simulation code with several simple geometries. Results of simulations were also compared to those of (Coulson et al. 1960), who have calculated the polarization arising from a plane-parallel atmosphere with Rayleigh scattering using Chandrasekhar functions. My simulations reproduced these results without difficulty.

### 3. Accretion disk models

In many persistent LMXB:s the inner disk and compact star have sufficient X-ray luminosity to keep the outer disk completely ionized. (King et al. 1997) This suppresses the thermal accretion disk instability (Tuchman et al. 1990). The Z sources are LMXB:s where the compact star is a neutron star and the accretion rate is probably close to Eddington limit (van der Klis 1989). In these systems the disk temperatures should be high enough to make electron scattering is the dominant opacity source (Frank et al. 1992). SXT:s in outburst have also completely ionized disks.

The vertical structure of accretion disks in LMXB:s is not very well known. It is often assumed that disks are very thin (Frank et al. 1992). However, this is not always a safe assumption (Shaviv et al. 1999). Irradiation may change the vertical disk structure (Dubus et al. 1999). Observations indicate that a thick disk is present at least in some LMXB:s (Mason 1989). Some X-ray (Hellier & Mason 1989) and optical (Hakala et al. 1999) observations are easiest to explain with asymmetric disks.

The standard disk model (see e.g. Frank et al. 1992) has gaussian vertical density profile if the disk is isothermal in vertical direction. The disks of LMXB:s are probably not very similar to standard disk model, as X-ray irradiation from the compact object may affect the disk structure. In my simulations the disk structure is needed only very near the disk surface, where the essential radiative transfer takes place. In contrast, the standard model is used to describe the entire disk and is most relevant at the disk plane, where most of the disk mass is. Disk models used in simulations have exponential vertical density profiles,  $\rho = \rho_0 \exp(-z/H)$ ,  $H = H(R, \phi)$ . The functional form of the scaleheight  $H$  may vary between disk models, but generally  $H = (H_0/R_0)R$ , where  $H_0/R_0$  is the ratio of scaleheight and radius at the inner disk. As variations in vertical density structure parameters do not produce significant variations in polarization, polarization is probably not very sensitive to the functional form of vertical density distribution.

Effects of the mass flow from the donor and tidal forces can cause deviations from axial symmetry in the disk. These are often observed, as most non-eclipsing LMXB:s show significant orbital variations in their optical brightness (Van Paradijs & McClintock 1995). Asymmetric models require binning of the photons in two dimensions. To obtain statistics comparable to that of axisymmetric simulations, the required processor capacity increases with a factor at least as large as the number of azimuth bins. Small-scale roughness of the disk surface, caused by turbulence, may be present. As the disk rotates with the binary and the gas moves in the disk, the Stokes parameters will be effectively azimuth-averaged in real observations.

Phase-resolved polarimetry has generally low signal-to noise ratio, as most LMXB:s have short periods and are very faint. Two simulations of non-axisymmetric disks with small-scale irregularities or warped disks were made. The Stokes parameters produced by simulations were azimuth-averaged to estimate the consequences of these effects.

Brightness temperature at the band in which polarization is measured and electron density are assumed to be proportional to powers of radius,  $T \propto R^\beta$ ,  $\rho \propto R^\gamma$ . The emission of the disk occurs in a layer near the disk surface, between two values of vertical optical depth,  $\tau_1$  and  $\tau_2$ . As the polarization of radiation emitted at  $\tau_z \geq 10$  is saturated, i.e. does not depend on emission depth, so  $\tau_1 = 10$  is a good upper limit. The dependence of polarization on  $\tau_1$  is quite weak for values near the saturation depth, as the polarization is close to the saturation value. Any values satisfying  $10 \geq \tau_1 > \tau_2 > 0$  can be used. Further constraints on the values can be derived by considering the X-ray irradiation, which is present in all LMXB:s. The X-rays come from the central source, so they will enter the disk from directions close to the tangent of the disk surface. A part of the X-rays is directly reflected, as others are captured by the gas. The absorption of X-rays is caused by photoelectric absorption and Compton scattering. The relative importance of these effects depends on the ionization states of different elements. Another complication is that the angle between the disk surface and incident X-rays is unknown. For accurate optical emission model, detailed information on the local disk structure and conditions and the X-ray emission geometry is needed. Instead of accurate physical modeling a crude zero-order approximation is used. The values used are  $\tau_1 = 5, 2$  and  $\tau_2 = 2, 1$ . These should not be very far from real values. The vertical optical depth,  $\tau_0$  at the inner disk edge is set to some value defined by setting  $z = 0$  and  $r = r_{in}$  in Eq. (4). The five free parameters ( $\beta, \gamma, \tau_0, \tau_1, \tau_2$ ) and the disk scaleheight  $H = H(R, \phi)$  define the disk model. As the opacity is produced by electron scattering only, opacity is directly proportional to density. When changing the parameter  $\gamma$ , also  $\tau_0$  must be changed to keep the disk optically thick at all radii.

As  $\tau_0, H$  and  $\gamma$  determine the density distribution, they represent total disk mass,  $M_{disk}$  and density at inner disk radius,  $\rho_{in} \cdot \rho_{in}$  can be derived from Eq. (4) and definition of  $\tau_0$ .

$$\tau_0 \equiv \int_0^\infty \kappa_r \rho(z, R_{in}) dz \Rightarrow \rho_{in} = 25 \frac{\tau_0}{H_{in}} \text{ kg m}^{-3} \quad (14)$$

where  $H_{in}$  is density scaleheight at inner disk in meters, and exponential vertical profile is assumed. The density can be directly integrated to get disk mass:

$$M_{disk} \approx 3.14 \cdot 10^8 \cdot \tau_0 R_{in}^2 \frac{X_{out}^{1+\gamma} - 1}{\gamma + 1} \text{ kg} \quad (15)$$

where  $X_{out}$  is the ratio of inner and outer disk radii, and  $R_{in}$  is inner disk radius in kilometers. If  $\gamma = 1$ , the fraction should be replaced with  $\ln(X_{out})$ . Setting  $R_{in} = 10 \text{ km}$  and  $\gamma = -2$  gives  $M_{disk} = 3.3 \cdot 10^{10} \tau_0 \text{ kg}$ . LMXB disk masses are not well known, but a rough estimate for the upper limit can be obtained assuming Eddington-limited accretion  $\dot{M} = 10^{15} \text{ kg s}^{-1}$  and accretion timescale of  $\Delta t = 10^5 \text{ s}$ , giving  $\Delta t \dot{M} = M_{max} =$

$10^{20}$  kg. The vertical optical depth at the outer disk edge is  $\tau_z = \tau_0 X_{\text{out}}^{\gamma+1}$ , and this should be larger than one to keep the disk optically thick even at the outer radii. This can be combined with the requirement of optically thick disk at all radii to yield  $\max(X_{\text{out}}^{-(\gamma+1)}, 1) < \tau_0 < 3 \cdot 10^9$ .

In most persistent LMXB:s the companion star has much smaller luminosity than the accretion disk. This is also true for SXT:s during the outburst. In some cases the secondary star is heated by X-rays from the compact star, which is observed as low-amplitude (generally below 0.2 magnitudes) ellipsoidal variations in the lightcurve. The electron scattering of the radiation from the secondary star may produce an additional polarization component. This effect can be significant in CV:s, but in persistent LMXB:s and SXT:s in outburst this should be a very small effect. In quiescent transients this effect is probably responsible for most of the polarization (Dolan & Tapia 1989). Electron scattering of the disk radiation by the secondary star should be insignificant, as the secondary stars in LMXB:s have low surface temperatures and therefore low free electron densities.

As the accuracy of polarization measurements does not allow accurate determination of the disk model, I used very simple disk models. All disk models used are axisymmetric or have azimuth-averaged Stokes parameters, and magnetic effects are ignored. As the polarization levels produced by electron scattering are quite small, other sources of polarization must also be considered.

The effects of magnetic fields, such as cyclotron or synchrotron radiation and disk disruption by magnetic field, are observed in some LMXB:s, e.g Her X-1. Many LMXB:s exhibit X-ray bursts indicating neutron star primaries with low magnetic field. Even in these systems the effect of the magnetic field can not be directly neglected. The magnetic field can cause the ionized gas emit elliptically polarized cyclotron/synchrotron radiation. Electron scattering in non-magnetic medium causes only linear polarization, but scattering in magnetic field produces elliptically polarized radiation (Whitney 1991), with larger effects in circular polarization. Magnetic field effects on scattering are most important when the frequency of the radiation is close to electron cyclotron frequency,  $\omega_c = qB/m_e$ . For optical light, this would require magnetic fields of order  $10^3$  T. The field strengths of neutron stars in disk-accreting LMXB:s can not be directly estimated, but propable LMXB endproducts, millisecond pulsars, have surface field strengths of the order  $10^4 - 10^5$  T (Bhattacharya 1995). It is also possible that some neutron stars in LMXB:s have even lower fields, as no magnetic effects are observed in some neutron star LMXB:s. For dipole field,  $B \propto R^{-3}$ , so magnetic effects are restricted to the innermost disk. The field could be temporarily screened by the accreted matter, reducing the magnetic effects further or suppressing them completely (Bhattacharya & Srinivasan 1995 and references therein). Measurements of circular polarization should be used to estimate the amount of linear polarization with magnetic origin in neutron star LMXB:s.

Differential saturation (Calamai et al. 1975) is an effect that produces pure linear polarization, when saturated absorption

**Table 1.** Parameters of simulated disk models

$\tau_0$	$\tau_1$	$\tau_2$	$\beta$	$\gamma$	$H/R$	Fig.
10000	5	2	-3/4	-2	0.005	1
5000	5	2	-3/4	-2	0.005	1
3000	5	2	-3/4	-2	0.005	1
2000	5	2	-3/4	-2	0.005	1,2
2000	5	2	-3/4	-2	0.015	2
2000	5	2	-3/4	-2	0.03	2
2000	5	2	-3/4	-2	0.06	2
2000	2	1	-3/4	-2	0.005	3
2000	2	1	-3/4	-2	0.015	3
2000	2	1	-3/4	-2	0.03	3
2000	2	1	-3/4	-2	0.06	3
2000	2	1	-1/2	-2	0.005	4
2000	2	1	-1/2	-2	0.015	4
2000	2	1	-1/2	-2	0.03	4
2000	2	1	-1/2	-2	0.06	4
3000	2	1	-3/4	-2	0.03	5
3000	2	1	-3/4	-2	$0.03(1 + 0.1\cos 10\phi)$	5
3000	2	1	-3/4	-2	$0.03(1 + 0.3\cos 10\phi)$	5
3000	2	1	-3/4	-2	$0.03(1 + 0.3\cos \phi)$	5
$3 \cdot 10^6$	2	1	$\beta(R)$	-2	0.005	6
$3 \cdot 10^6$	2	1	0	-2	0.005	7
$3 \cdot 10^6$	2	1	-1	-2	0.005	8

lines are Zeeman-split. In a typical LMXB spectrum most lines are in emission, so differential saturation from the disk can be safely neglected. In VY Scl stars, also known as anti-dwarf novae, most of the accretion disk is also ionized, and only the outermost parts of the disk may be neutral (Leach et al. 1999). In these systems the accretion rate shows long-term variations. Two explanations for this have been presented: shielding of the secondary by the accretion disk rim (Wu et al. 1995) and a magnetic mechanism, where starspots of the secondary close to the inner Lagrange point reduce the accretion flow (Livio & Pringle 1994). The latter scenario assumes that the secondary has a high surface magnetic field. CV secondaries are late-type stars with many absorption lines, and the secondary contribution to the optical luminosity may be significant. Therefore differential saturation may cause linear polarization in VY Scl stars. In some cases, the polarization produced by differential saturation may cancel some of the polarization produced by Thomson scattering (Huovelin 1990). If my results are applied to these systems, the polarization produced by differential saturation should be carefully estimated.

#### 4. Results

The number of free parameters needed to define a disk model is large enough to make extensive mapping of the parameter space practically impossible. Some of these parameters can not be deduced from observations or constrained theoretically. Fortunately, most of the parameters do not influence the polarization levels when physical values are used. Simulated disk models are listed in Table 1. The errors of all axisymmetric simulations are smaller than 0.02% for inclinations above  $20^\circ$  and smaller than

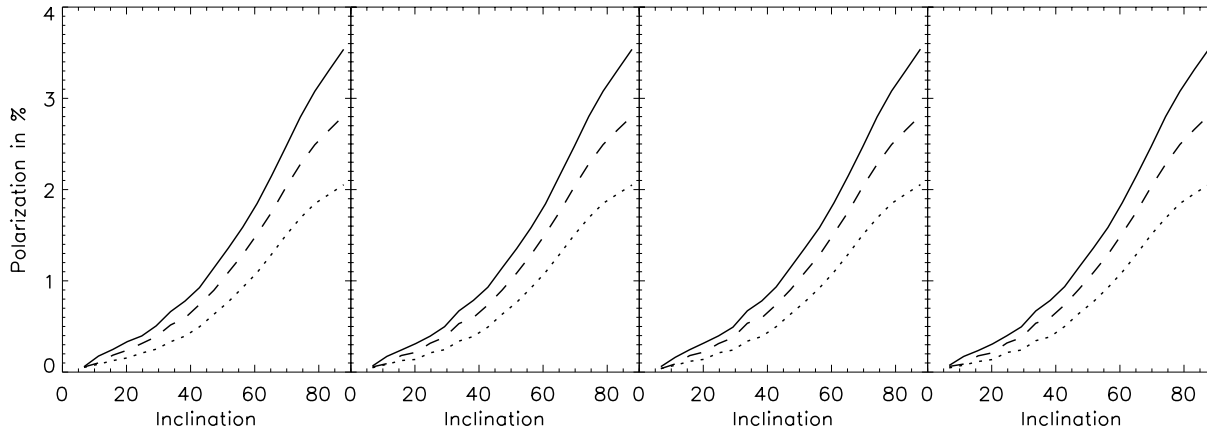


**Fig. 1.** Polarization from a thin, viscous disk. Vertical optical depth  $\tau_0$  at the inner disk from the left: 10000, 5000, 3000 and 2000. Solid line: only single scattering, dashed line: double scattering included, dotted line: multiple scattering included.

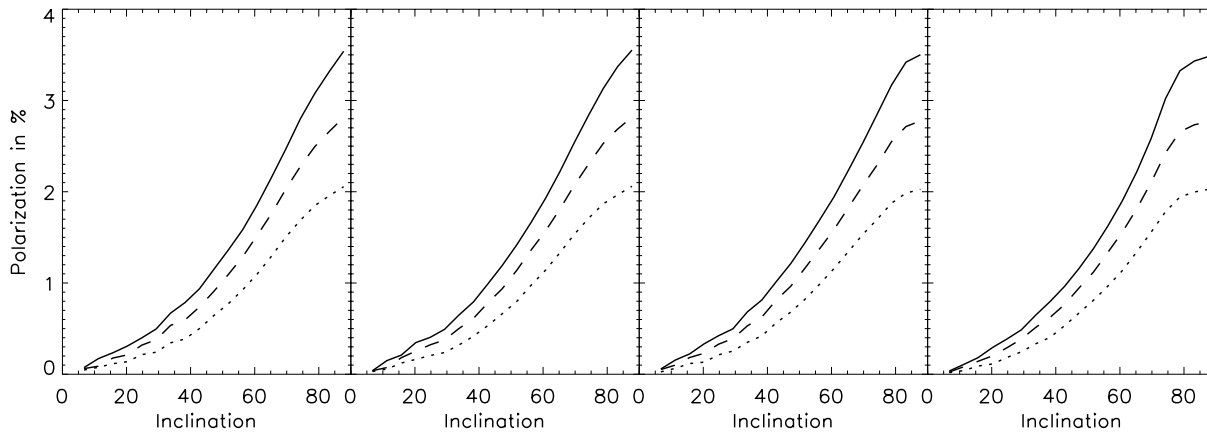


**Fig. 2.** Polarization from a viscous disk. Disk parameters are  $\beta = -3/4$ ,  $\gamma = -2$ ,  $\tau_0 = 2000$ ,  $\tau_1 = 2$  and  $\tau_2 = 5$ . The disk scaleheights are from the left  $0.005R$ ,  $0.015R$ ,  $0.03R$  and  $0.06R$ . Solid line: only single scattering, dashed line: double scattering included, dotted line: multiple scattering included.

0.05% for inclinations below  $20^\circ$ . Error bars have been left out of the figures for clarity.

The parameters of the disks modeled in Fig. 1 are  $\beta = -3/4$ , corresponding to standard viscously heated disk,  $\gamma = -2$ ,  $H = 0.005R$ ,  $\tau_1 = 2$  and  $\tau_2 = 5$ . The disks are thin, and radiation is generated not very near the disk surface.  $\tau_0$  parameter (vertical optical depth at the inner disk) varies between 10000 and 2000. As the vertical optical depth decreases outward, the lowest value corresponds to a disk which is optically thin in the outer parts. As the emissivity of the disk is proportional to  $T^4 \propto R^{-3}$ , ( $\beta = -3/4$ ), the contribution of the outer disk to the radiation is negligible. Consequently, the outer disk radius has no effect in polarization. The results shown in Fig. 1 clearly show that the vertical optical depth of the disk has no large effects on polarization. Therefore disk mass or accretion rate can not be estimated from polarization observations. The polarization levels are easily observable for brightest LMXBs, if their inclination is above  $20^\circ$ . The disk rim is not modelled correctly, as the disk is only cut off at a sufficiently large radius. Therefore our simulations have only marginal significance for eclipsing systems, where a large fraction of the observed optical

flux comes from the outer disk. The simulations are more relevant to medium and low inclination systems ( $i > 60^\circ$ ), where the inner disk produces most of the observed flux.

Fig. 2 shows results for a viscous disk where the disk scaleheight is varied. The fixed disk parameters are  $\beta = -3/4$ ,  $\gamma = -2$ ,  $\tau_0 = 2000$ ,  $\tau_1 = 2$  and  $\tau_2 = 5$ . The disk scaleheight varies from  $H = 0.005R$  to  $H = 0.06R$ . The effect of increasing thickness is observable at high inclinations, where the disk rim modelling should be more detailed to produce reliable results. No effect in polarization levels is seen at lower inclinations. In Figs. 3 and 4 results for irradiated (X-ray heated) disks, are shown. These disks are similar to the viscous disks in Fig. 2, but the radiation is generated closer to the disk surface. The radial emissivity profile of disks in Fig. 3 is the same as those in Fig. 2 ( $T_\nu \propto R^{-3/4}$ ), whereas for Fig. 4 the emissivity profile is less steep ( $T_X \propto R^{-1/2}$ ). The hybrid models of Fig. 3 with radial temperature distribution of a viscous disk and vertical emissivity distribution of an irradiated disk were simulated to allow separation between the effects of both radial and vertical emissivity variations on polarization. The optical luminosity of a real disk is a sum of the released gravitational potential en-

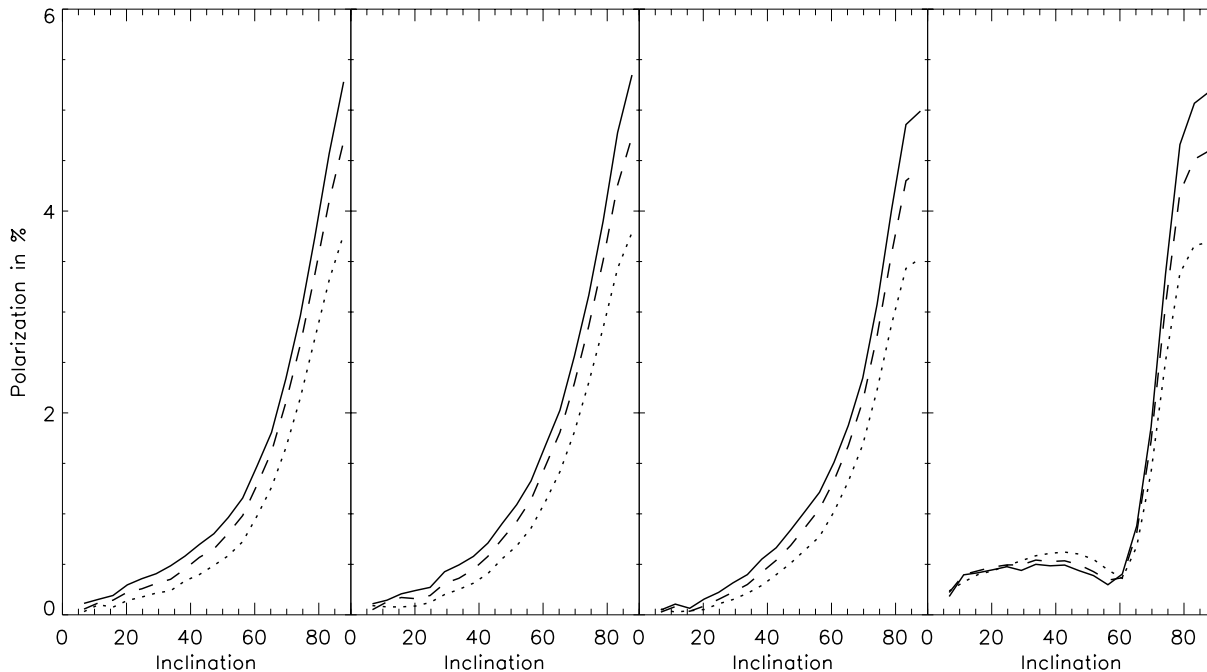


**Fig. 3.** Polarization from a lightly irradiated disk. Disk parameters are  $\beta = -3/4$ ,  $\gamma = -2$ ,  $\tau_0 = 2000$ ,  $\tau_1 = 1$  and  $\tau_2 = 2$ . The disk scaleheight  $H$  is from the left:  $0.005R$ ,  $0.015R$ ,  $0.03R$ , and  $0.06R$ . Solid line: only single scattering, dashed line: double scattering included, dotted line: multiple scattering included.

ergy and the energy of the compact object X-rays absorbed in the disk surface layers, so the real radial dependence of emissivity is roughly  $T(R)^4 = T(R)_X^4 + T(R)_V^4$ , so the value of  $\beta$  is between  $-1/2$  and  $-3/4$ , and  $\beta = \beta(R)$ . The somewhat arbitrary division between different emissivity profiles is motivated by the fact Stokes parameters are additive. Therefore results of the simulations are also additive, if parameters  $\beta$ ,  $\tau_1$  and  $\tau_2$  are changed and other parameters, which describe the distribution of the electrons, are kept constant. Specially, simulations of different emission mechanisms, such as those presented in Figs. 2, 3 and 4, can therefore be combined to give a more realistic polarization model.

The fixed disk parameters are  $\gamma = -2$ ,  $\tau_0 = 2000$ ,  $\tau_1 = 1$  and  $\tau_2 = 2$  for both figures. The lower values of  $\tau_1 = 1$  and  $\tau_2 = 2$  are chosen to model the irradiated disk, as the energy absorbed from X-rays will be emitted closer to the disk surface. The parameter  $\beta$  is set to  $-3/4$  for Fig. 3 and to  $-1/2$  in the I band compared to UBVR in polarimetric observations of Her X-1 (Egonsson & Hakala 1991). The depths where of different emission lines are formed could perhaps be deduced from spectropolarimetric observations, but this is not possible with present instruments and telescopes.

The low viscosity of gas in accretion disks probably causes turbulence (Frank et al. 1992). In turbulent disks, small-scale irregularities may be present. Irregularities of emission and scattering regions cause reduction in the polarization, as directions of polarization vectors have larger variations, and therefore larger fraction of polarization is cancelled. Small-scale irregularities were modelled by varying the disk scaleheight with azimuth. Azimuth-integrated results for these disks are presented in Fig. 5, where all disks have parameters  $\beta = -3/4$ ,  $\gamma = -2$ ,

tical thickness and scaleheight of medium-inclination systems can not be derived from polarization observations. Conversely, no information of disk thickness or scaleheight is needed when inclination estimates are derived from polarization observations. However, it is challenging to distinguish effects caused by inclination from those related to the vertical structure.

The results of Figs. 2, 3 and 4 show clearly, that polarization levels are quite sensitive to the vertical temperature profile. Radial temperature profile has a smaller effect on polarization, and other parameters do not produce observable effects, if the disk is thin. This has two important observational consequences: As the color temperatures corresponding to different wavelengths have variable radial dependence, they should also have different polarization levels. This effect could perhaps be seen if polarization measurements were carried out at different wavebands, and it may be responsible for the lower S/N ratio in the I band compared to UBVR in polarimetric observations of Her X-1 (Egonsson & Hakala 1991). The depths where of different emission lines are formed could perhaps be deduced from spectropolarimetric observations, but this is not possible with present instruments and telescopes.

The low viscosity of gas in accretion disks probably causes turbulence (Frank et al. 1992). In turbulent disks, small-scale irregularities may be present. Irregularities of emission and scattering regions cause reduction in the polarization, as directions of polarization vectors have larger variations, and therefore larger fraction of polarization is cancelled. Small-scale irregularities were modelled by varying the disk scaleheight with azimuth. Azimuth-integrated results for these disks are presented in Fig. 5, where all disks have parameters  $\beta = -3/4$ ,  $\gamma = -2$ ,

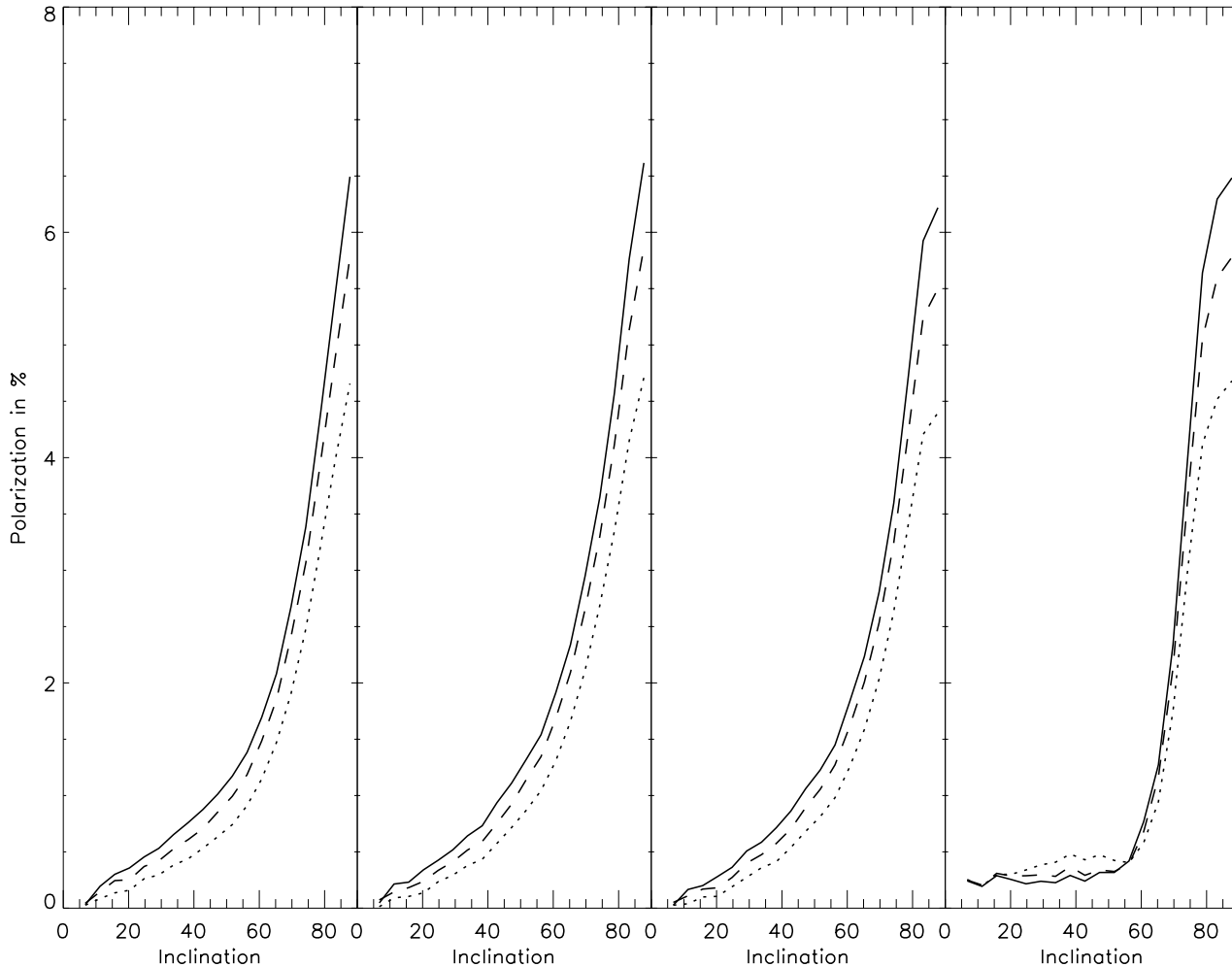


**Fig. 4.** Polarization from a heavily irradiated disk. Disk parameters are  $\beta = -1/2$ ,  $\gamma = -2$ ,  $\tau_0 = 2000$ ,  $\tau_1 = 1$  and  $\tau_2 = 2$ . The disk scaleheight  $H$  is from the left:  $0.005R$ ,  $0.015R$ ,  $0.03R$  and  $0.06R$ . Solid line: only single scattering, dashed line: double scattering included, dotted line: multiple scattering included.

$\tau_0 = 3000$ ,  $\tau_1 = 1$  and  $\tau_2 = 2$ . The disk in the first panel on the left has  $H = 0.03R$ , corresponding to a regular disk. In the two following panels,  $H = 0.03R(1 + 0.1 \cos 10\phi)$  and  $0.03R(1 + 0.3 \cos 10\phi)$ . These disks have a little lower polarization levels, as expected. The irregularities in these models have small size, so time resolution of polarization observations is not sufficient to observe real variations of polarization. Only cancellation of polarization due to more random polarization directions is observed. The rightmost panel has  $H = 0.03R(1 + 0.3 \cos \phi)$ , approximating a warped disk. Warped disks are a possible explanation for long-term photometric variations seen in some X-ray binaries (Pringle 1996).

Some simulations of disks with gaussian vertical density profile and with disk models having different radial density profiles,  $\gamma = -1.5$  or  $\gamma = -2.5$  were made. The results were almost identical to those shown in previous figures, so  $\gamma$  and vertical profile do not have large influence on polarization. The evaluation of integrals with gaussian profiles is more complicated than that of exponentials. This increases the required computing time with almost one order of magnitude.

## 5. Application example: Scorpius X-1

Scor X-1 is the brightest LMXB with  $B \simeq 12$ , making it a good candidate for optical/UV polarization measurements. On the basis of its X-ray timing properties it is classified as a Z source, indicating neutron star primary and near-Eddington accretion rate (Hasinger & van der Klis 1989). X-ray timing analysis shows also that magnetic field of the neutron star is extremely low (van der Klis et al. 1997), so the inner disk radius is  $\simeq 10$ km. The mass accretion rate ( $\dot{M}$ ), outer disk radius ( $R_{\max}$ ) and fraction of X-rays absorbed to the accretion disk ( $f_X$ ), have been estimated from IUE observations (Kallman et al. 1991), giving  $\dot{M} = 0.3 - 1.1 \cdot 10^{15} \text{kg s}^{-1}$ ,  $R_{\max} = 0.24 - 2.43 \cdot 10^8 \text{m}$  and  $f_X = 0.6 - 7.2 \cdot 10^{-3}$ . The inclination of the system is quite low, most probably below  $\sim 30^\circ$  (Crampton et al. 1976). The temperature of the disk is affected by both viscous energy release and X-ray irradiation, so the real temperature profile is

$$T^4 = T_X^4 + T_\nu^4 = \frac{\eta \dot{M} c^2 f_X}{4\pi\sigma R^2} + \frac{3GM\dot{M}}{8\pi\sigma R^3} \quad (16)$$

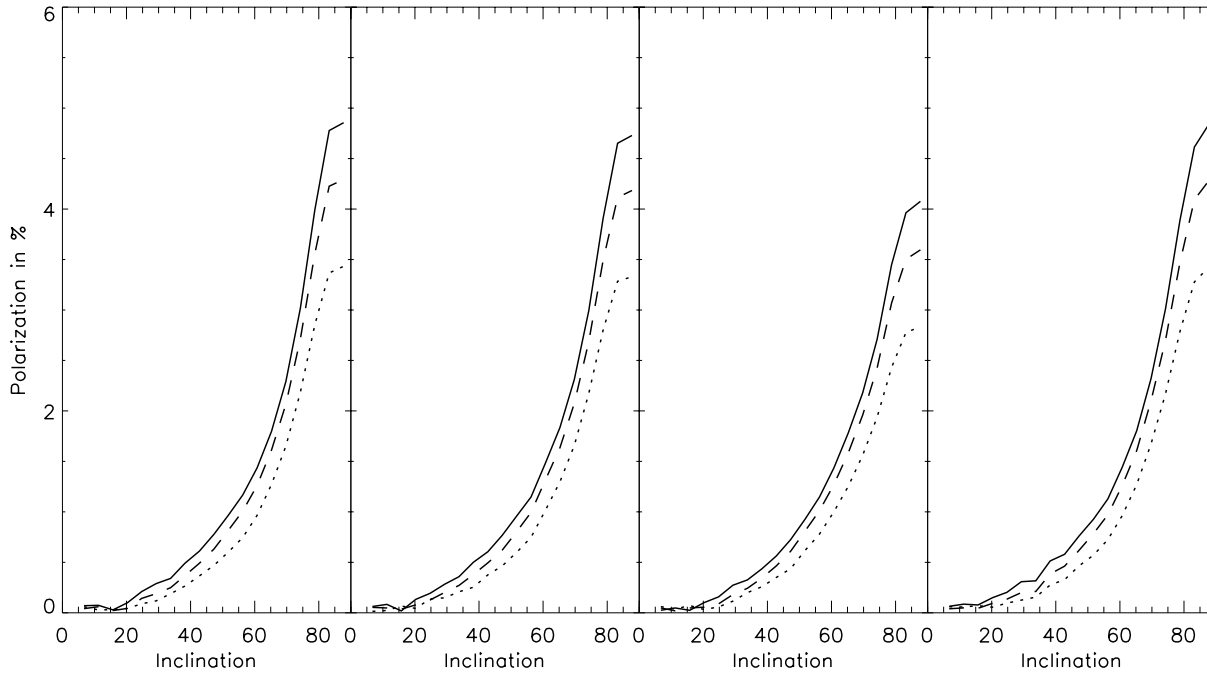


**Fig. 5.** Polarization from irregular disks. Disk parameters are  $\beta = -3/4$ ,  $\gamma = -2$ ,  $\tau_0 = 3000$ ,  $\tau_1 = 1$  and  $\tau_2 = 2$ . First panel on the left, a regular disk ( $H = 0.03R$ ) for comparison, Second panel: ( $H = 0.03R(1 + 0.1 \cos(10\phi))$ ), Third panel: ( $H = 0.03R(1 + 0.3 \cos(10\phi))$ ), Fourth panel: Warped disk, ( $H = 0.03R(1 + 0.3 \cos \phi)$ ) Solid line: only single scattering, dashed line: double scattering included, dotted line: multiple scattering included.

where  $\eta \approx 0.1$  is an efficiency factor and other symbols have their usual meanings. Setting  $R_{\text{in}} = 10\text{km}$ ,  $f_X = 10^{-3}$  and  $\dot{M} = 10^{15}\text{kg s}^{-1}$  in Eq. (16) we get

$$T = 2.3 \cdot 10^7 (R/R_{\text{in}})^{-3/4} \left(1 + \frac{R}{18000R_{\text{in}}}\right)^{1/4} \text{ K} \quad (17)$$

X-ray irradiation is important for the temperature profile in the outer disk. At the outer edge of the disk, the temperature is  $T \approx 10^4\text{K}$ , so the entire disk should be ionized. The optical luminosities derived from this model are a few times larger than those observed (Kallman et al. 1991). The values of  $\tau_0 = 3 \cdot 10^6$ ,  $\tau_1 = 1$ ,  $\tau_2 = 2$  and  $H = 0.005 R/R_0$  were adopted. The simulations predict small but observable polarization values for Sco X-1. (Fig. 6). No significant wavelength dependence is seen from the results. More detailed modelling of the disk rim and opacity in the cooler disk regions could result to lower polarization levels in the longest wavelengths, as some of the scattered radiation in the outer disk would be absorbed. Similar polarization values could be obtained from Fig. 4. To estimate the polarization variations caused by radial temperature profile, simulations with other temperature profiles were made. Of the two models used, one has constant disk temperature, which should be a rough estimate of a disk heated by scattering from the corona (ADC-model). The other model had a steep temperature profile,  $T \propto R^{-1}$ . The inner disk temperature is same as in the model for Sco X-1. The results are represented in Fig. 7 and Fig. 8. No significant change in value or wavelength dependence of polarization is seen with steeper temperature profile. As the temperature profile effects on polarization are minimal, the ra-

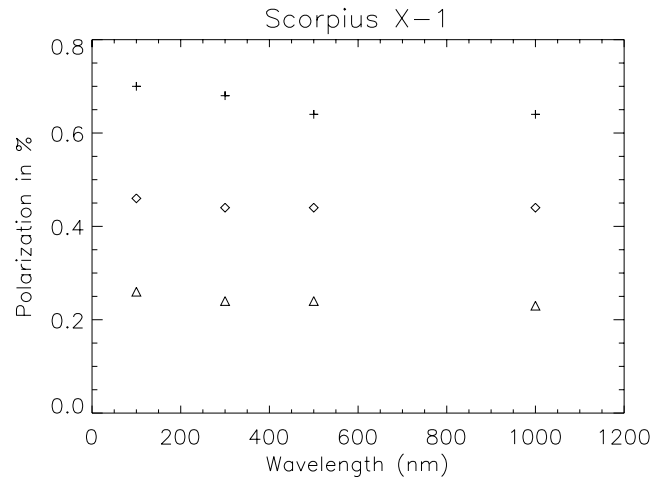


**Fig. 6.** Linear polarization vs. wavelength. Simulation for Scorpius X-1, assuming axisymmetric pure electron scattering disk. Crosses, diamonds and triangles correspond to inclination values of  $30^\circ$ ,  $20^\circ$  and  $10^\circ$

dial structure of the disk does not influence polarization, and no detailed information on the radial disk structure is needed for the interpretation of observations.

## 6. Discussion and conclusions

I have estimated linear polarization levels of pure electron scattering accretion disks using the Monte Carlo method. The simulations produce linear polarization levels of order 1% for the

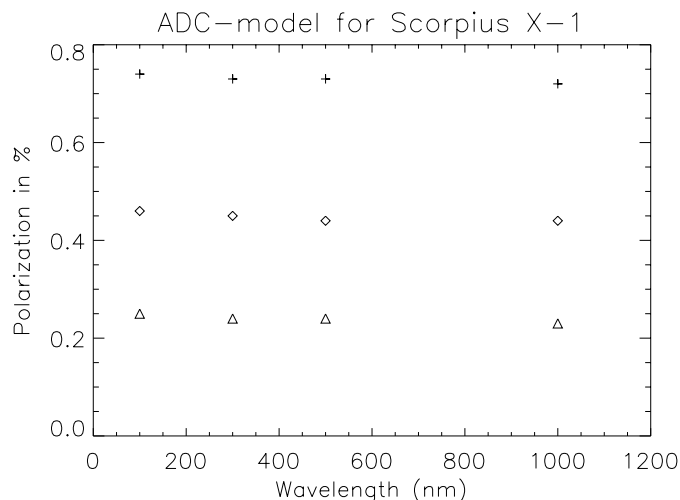


**Fig. 7.** Linear polarization vs. wavelength. Simulation for the density distribution of Fig. 6, with constant disk temperature ( $\beta = 0$ ). Crosses, diamonds and triangles correspond to inclination values of  $30^\circ$ ,  $20^\circ$  and  $10^\circ$

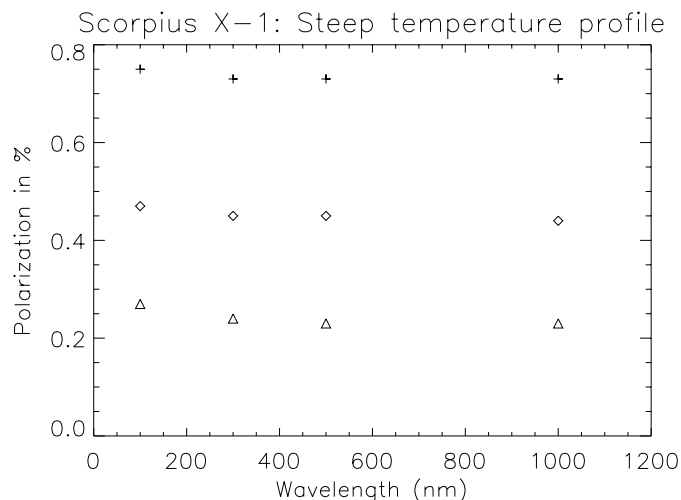


**Fig. 8.** Linear polarization vs. wavelength. Simulation for the density distribution of Fig. 6, with steep temperature profile ( $\beta = -1$ ). Crosses, diamonds and triangles correspond to inclination values of  $30^\circ$ ,  $20^\circ$  and  $10^\circ$

bolometric flux. As most of the accretion disk luminosity is released in UV wavelengths, polarization levels of this order may be expected in these wavelengths. In optical light, the polarization levels might be a little lower due to flatter color temperature profiles. The effect of small-scale azimuthal asymmetries to azimuth-averaged Stokes parameters was also estimated, and found relatively small. Large-scale asymmetries may be observed as polarization variations with the orbital period. Orbital variations of polarization can be studied only in a few brightest X-ray binaries.

Single-scattering approximation should not be used when modeling the polarization of accretion disks, as it produces significantly larger polarization levels than multiple-scattering models. Decreasing polarization with multiple scattering is also seen in a plane-parallel atmosphere, when polarization is evaluated from Chandrasekhar functions (Coulson et al. 1960). The geometry of accretion disk is similar to that of Coulson et al., so qualitatively similar results are produced. In Be star disks, simulations indicate increasing polarization with multiple scattering (Wood et al. 1996). This does not contradict my results, as the source of radiation is the central star in Be star disks, and the disk itself in LMXB accretion disks.

The polarization level produced by a disk is sensitive to vertical distribution of emissivity, and no dependence on the distribution of absorbing gas or radial temperature profile is seen. This eliminates several dimensions from the parameter space, so the interpretation of observations is easier than expected from the amount of free parameters. As the radial structure of accretion disks is generally better known than vertical, it is important to note that polarization is more sensitive to vertical structure. In principle spectropolarimetric observations could be used to estimate the inclination and vertical emissivity distribution of an accretion disk, but more detailed studies of this are required. Spectropolarimetric observations of LMXB:s may be useful in estimating the emission region of the disk.

The disk models used in simulations are probably relevant to two types of LMXB:s, SXT:s in outburst and Z sources. The disks of VY Sculptoris-type CV:s are also probably similar to the simulated models, but the radiation of the secondary star should be included to the model. Irregularities in disks may reduce the polarization.

Better polarization estimates can be obtained, if other opacity sources and deviations from axial symmetry are taken into account. This is particularly important for CV:s. Both linear and circular polarization of the disk should be measured to avoid confusion between polarization components produced by electron scattering and magnetic effects. This is especially important in neutron star LMXB:s.

*Acknowledgements.* I wish to thank P. Hakala, J. Huovelin, K. Muinonen, O. Vilhu and the referee, K. Wood, for their constructive criticism and useful comments. This research was supported by the Space Research Programme at University of Helsinki Observatory, supported by Academy of Finland. This research has made use of NASA's Astrophysics Data System Bibliographic Services.

## References

- Bhattachaya D., 1995, In: Lewin W.H.G., van Paradijs J., van den Heuvel E.P.J. (eds.) X-ray Binaries. Cambridge University Press
- Bhattachaya D., Srinivasan G., 1995, In: Lewin W.H.G., van Paradijs J., van den Heuvel E.P.J. (eds.) X-ray Binaries. Cambridge University Press
- Bianchi S., Ferrara A., Giovanardi C., 1996, ApJ 465, 127
- Calamai G., Landi Degl'Innocenti E., Landi Degl'Innocenti M., 1975, A&A 45, 297
- Cashwell E.D., Everett C.J., 1959, A Practical Manual on the Monte Carlo Method for Random Walk Problems. Pergamon Press
- Coulson K.L., Dave J.V., Sekera Z., 1960, Tables Related to Radiation Emerging from a Planetary Atmosphere with Rayleigh Scattering
- Crampton D., Cowley A., Hutchings J.B., et al., 1976, ApJ 207, 907
- Dolan J.F., Tapia S., 1989, PASP 101, 1135

- Dubus G., Lasota J.-P., Hameury J.-M., et al., 1999, MNRAS 303, 139
- Egonsson J. Hakala P., 1991, A&A 244, L41
- Frank J., King A.R., Raine D., 1992, *Accretion Power in Astrophysics*. 2nd ed., Cambridge University Press
- Hakala P.J., Muhli P., Dubus G., 1999, MNRAS 306, 71
- Hasinger G., van der Klis M., 1989, A&A 225, 79
- Hellier C., Mason K.O., 1989, MNRAS 239, 715
- Huovelin J., 1990, Thesis, Report 4/90 of Observatory at University of Helsinki, Finland
- Kallman T.R., Raymond J.C., Vrtilik S.D., 1991, ApJ 370, 717
- King A.R., Kolb U., Szuszkiewicz E., 1997, ApJ 488, 89
- Leach R., Hessman F.V., King A.R., et al. 1999, MNRAS 305, 225
- Livio M., Pringle J.E., 1994, ApJ 427, 956
- Mason K., 1989, In: Hunt J., Battrick B. (eds.) Proc. 23rd ESLAB Conference on X-ray Astronomy Vol. 1, X-ray binaries. ESA, Paris, p. 185
- Pringle J.E., 1996, MNRAS 281, 357
- Shakhovskoi N.M., Efimov Yu.S., 1975, In: Sherwood V.E., Plaut L. (eds.) IAU Symposium 67, Variable Stars and Stellar Evolution. Kluwer
- Shaviv G., Wickramasinghe D., Wehrse R., 1999, A&A 344, 639
- Tuchman Y., Mineshige S., Wheeler J.C., 1990, ApJ 359, 164
- van Paradijs J., McClintock J.E., 1995, In: Lewin W.H.G., van Paradijs J., van den Heuvel E.P.J. (eds.) X-ray Binaries. Cambridge University Press
- van der Klis M., 1989, ARA&A, 517
- van der Klis M., Wijnands R.A.D., Horne K., et al., 1997, ApJ 481, L97
- Whitney B.A., 1991, ApJS 75, 1293
- Wood K., Bjorkman J.E., Whitney B.A., et al., 1996, ApJ 461, 828
- Wu K., Wickramasinghe D.T., Warner B., 1995, Proc. Astron. Soc. Aust. 12, 60